Reaktor

p-ISSN 0852 – 0798
e-ISSN 2407 – 5973

Website: http://ejournal.undip.ac.id/index.php/reaktor/

Reaktor, Vol. 25 No. 2, August Year 2025, pp. 81-89

Sulfonated Polysulfone/PEG/Halloysite Nanotube Hybrid Tight-Ultrafiltration Membranes for Treatment of Industrially Contaminated Raw Water

Jessica Enis Okinawa[1)], Diva Amerya Agustin[1)], Rani Annisa[1)], Tiara Ariani Putri[1)], and Putu Teta Prihartini Aryanti[1,*)]

[1)]Department of Chemical Engineering, Faculty of Engineering, Universitas Jenderal Achmad Yani
Jl. Terusan Jenderal Sudirman, Cimahi, Indonesia

[*)] Corresponding author: p.teta@lecture.unjani.ac.id

(Received: 25 September 2025; Accepted: 14 November 2025; Published: 25 November 2025)

Abstract

The quality of river water in Indonesia predominantly falls below the established standards for clean water, including the Citarum River in West Java. Despite the associated health risks, many residents in the river basin continue to utilize this water for their daily needs. This study aims to develop tightly structured ultrafiltration membranes (tight-UF) capable of treating contaminated raw water into clean water. The tight-UF membranes were fabricated using sulfonated polysulfone (SPSf, 20 wt.%), blended with polyethylene glycol (PEG400, 20 wt.%), and halloysite nanotube additives (HNT, 1-2 wt.% in a solvent mixture of acetone and dimethylacetamide (Ac/DMAc). SPSf was synthesized using a sulfonation technique involving immersion in sulfuric acid, with purities of 70 wt.% and 98 wt.%. Experimental results demonstrated that a higher acetone content reduced membrane porosity and increased skin layer thickness. Additionally, excessive loading of HNT (2 wt.%) caused particle agglomeration and decreased selectivity. In contrast, a moderate addition of HNT (1 wt.%) enhanced both hydrophilicity and structural integrity. The optimized formulation, comprising SPSf/PEG400/HNT/Ac 20/20/1/6 wt.% with 98 wt.% sulfonation, achieved an impressive rejection rate of 98.57% and a stable water flux of 63.45 $L \cdot m^{-2} \cdot h^{-1}$. These findings emphasize the potential of SPSf-based tight-UF membranes as a robust and energy-efficient solution for sustainable clean water production from contaminated surface water sources.

Keywords: contaminated raw water, ultrafiltration membrane, sulfonated polysulfone, clean water

How to Cite This Article: Okinawa, J.E., Agustin, D.A., Annisa, R., Putri, T.A., Aryanti, P.T.P. (2025), Sulfonated Polysulfone/PEG/Halloysite Nanotube Hybrid Tight-Ultrafiltration Membranes for Treatment of Industrially Contaminated Raw Water, *Reaktor*, 25 (2), 81–89, https://doi.org/10.14710/reaktor.25.2.81-89

INTRODUCTION

Indonesia has been facing a tremendous issue in terms of freshwater resources in the last few decades. Rapid industrialization, population growth, and inadequate wastewater management have led to severe pollution in waterways across the country. The data from the Directorate General of Pollution and Environmental Damage Control indicate that only about 5.3% of rivers meet water quality standards, while 59% are categorized as extremely polluted, 26.6% as

moderately polluted, and 8.87% as slightly polluted (Basuki *et al*., 2024). The extent of pollution is particularly concerning during the dry season, when reduced surface water and insufficient clean water supplies force riverbank populations to utilize contaminated river water for their daily needs (Chakraborty, 2021). This reliance presents significant health hazards due to heightened levels of chemical and organic contaminants. Consequently, there is an immediate necessity for efficient water treatment technology that is able to transform polluted river water into safe and usable water for impacted communities.

One promising technology in addressing these challenges is tight-structured ultrafiltration (tight-UF) membranes (Siagian *et al*., 2021). These membranes exhibit higher selectivity to dissolved compounds. such as humics and dyes (over 85%) than conventional UF membranes (Aryanti *et al*., 2018) and operate at lower pressures (1–2 bar) than nanofiltration (NF) and reverse osmosis (RO) (over 5 bar) (Xiang *et al*., 2022). These advantages make tight-UF membranes increasingly attractive, especially in applications for the removal of dissolved compounds in water.

Wang *et al*. (2020) fabricated a tight-UF membrane through polymerization on the surface of a porous polysulfone (PSf) membrane, forming a covalent organic framework composite layer. Despite having a high permeate flux (66 $L \cdot m^{-2} \cdot h^{-1}$) and color rejection of up to 99%, this polymerization technique is still complicated in industrial-scale manufacturing, and the membrane structure is not uniform (Xie *et al*., 2023). Aryanti et al. (2022) made UF membranes with an easier technique, namely mixing PSf, polyethylene glycol (PEG400), ZnO, and acetone. However, the color rejection was still low, at 45%, with a flux of 60 $L \cdot m^{-2} \cdot h^{-1}$. Efforts to improve membrane performance can be focused on the introduction of other additives that can increase both the flux and the rejection rate of contaminants in raw water.

One interesting additive is halloysite nanotubes (HNT) (Figure 1), which have the potential to improve the selectivity of tight-UF membranes (de Oliveira and Beatrice, 2018). HNTs have a multilayered structure with the outer surface coated by siloxane functionalities (Si-O-Si) and Al-OH groups, offering a high surface area and optimal surface interaction (Choi *et al*., 2022). In addition, the nature of the negative charge on the outer surface and the positive charge on the inner surface makes HNTs have desirable antifouling characteristics (Katana *et al*., 2020). Providing a negative charge on the surface and structure of the membrane through sulfonation techniques also has the potential to increase the membrane's ability to reject organic compounds and dyes present in raw water.

In this study, a UF membrane was prepared from PSf by giving a negative charge to polysulfone through the sulfonation technique (SPSf). SPSf was

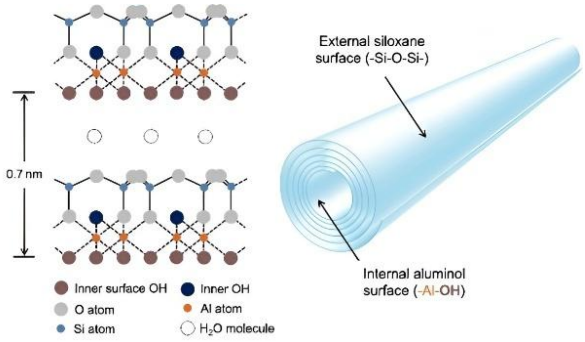

Figure 1. Structure of halloysite nanotube (HNT) molecules (de Oliveira and Beatrice, 2018)

immersed in sulfuric acid (H_2SO_4), with purities of 70 wt% and 98 wt.%.Tight-UF membranes were developed by mixing polymers, namely SPSf and polyethylene glycol (PEG400), with various variations of HNT nanoparticles, and using acetone and dimethylacetamide (DMAc) as solvents. This research is expected to produce a tight UF membrane with high rejection ability and antifouling properties, allowing it can be applied for the treatment of polluted raw water into clean water that is safe to use.

RESEARCH METHOD

Materials

Polysulfone (UDEL P-3500 MB, MW of 77,000-83,000 $g \cdot mol^{-1}$) was purchased from Solvay Advanced Polymers. N, N-dimethylacetamide (purity of 99.9%) was provided by Shanghai Jingsan Jingwei Chemical Co. Ltd. The HNT ($Al_2H_4O_5Si$, average diameter of 30 – 50 nm, molecular weight of 258.16 $g \cdot mol^{-1}$) was supplied by Nano Research Elements. Meanwhile, acetone (analysis Merck) and polyethylene glycol (PEG400) were obtained from a local supplier (Kimia Jaya, Semarang). The raw water was sourced from one of the contaminated rivers in Bandung city without any prior treatment.

Synthesis of Sulfonated Polysulfone (SPSf)

Sulfonation was carried out by immersing granular PSf in sulfuric acid (Al, 70 and 98 wt.%) for 5 hours at a constant temperature of 70°C. The ratio of SPSf:H_2SO_4 was 1:5. The sulfonated PSf was then removed from the acid solution and washed several times with demineralized water to remove excess H_2SO_4. The amount of negative charge (sulfonate groups, HSO_3^-) in the UF membrane structure was determined by the ion exchange capacity (IEC) value, which was calculated by the back-titration method (Akli *et al*., 2016). Dried SPSf (0.3 g) was soaked in 30 mL of 2 M NaCl solution for 24 hours at room temperature. The amount of H^+ ions released in the solution was measured by the titration method in a 0.01 M standard NaOH solution and phenolphthalein as an indicator. The IEC ($mmol \cdot g^{-1}$) was calculated using Equation (1) as follows:

$$IEC = \frac{C_{NaOH} \times V_{NaOH}}{W_p} \quad (1)$$

where C_{NaOH} is the NaOH concentration (mM or mmol·mL^{-1}), V_{NaOH} is the volume of NaOH (mL) required until the equivalence point is reached, and W_p is the dry polymer weight (g). Meanwhile, the degree of sulfonation (DS, %) was calculated based on Equation (2) (Tang et al., 2020). The molar masses of the PSf repeating unit and the sulfonate group (SO_3) are 442.52 (Kalkhoran, 2015) and 80 g·g-mol^{-1} *(Tang et al*., 2020).

$$DS = \frac{442.52 \times IEC}{1000 - (80 \times IEC)} \times 100\% \quad (2)$$

Fabrication of Flat-sheet Tight-UF Membrane

The tight-UF sheet membrane was prepared using the immersion precipitation method. The preparation steps are displayed in Figure 2. SPSf, PEG400, and HNT were mixed in a solvent containing DMAc and acetone. The concentration of SPSf and PEG400 was 20 wt.%, while the concentration of acetone varied from 0 to 6 wt.%. HNT was added to the membrane solution at a concentration of 1 wt.% of the total polymer weight (SPSf and PEG400). The membrane solution was stirred for 24 hours until it became homogeneous and stopped until all bubbles in the solution had disappeared. The homogeneous membrane solution was printed on flat glass with a membrane thickness of 150 µm and immediately immersed in a coagulation bath containing distilled water at room temperature (± 26°C). After the membrane was detached from the flat glass, the tight-UF membrane was soaked in another coagulation bath for 24 hours to allow complete evaporation of the solvents. The tight-UF membrane sheet was cut into a circle shape with a diameter of 9 cm, and then installed on the membrane module for flux testing.

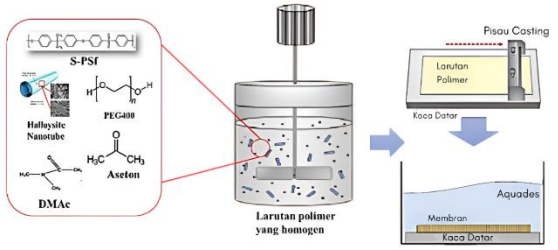

Figure 2. Stages of the Manufacturing Process of SPSf/PEG400/HNT/ AC/DMAc-based Tight-UF Membrane

Measurement of Permeate Flux and Rejection

Flux test was carried out by passing pure water through the tested membrane, as shown in Figure 3, and calculated with the equation below:

$$J = \frac{V}{A \times t} \quad (3)$$

where J is the permeate flux (L·m^{-2}·h^{-1}), V is the permeate volume (L), A is membrane area (m^2), and t is the operation time (h). Ultrafiltration of raw water polluted with industrial effluents was carried out for 60 minutes (1 hour). The permeating flux was measured every 20 minutes.

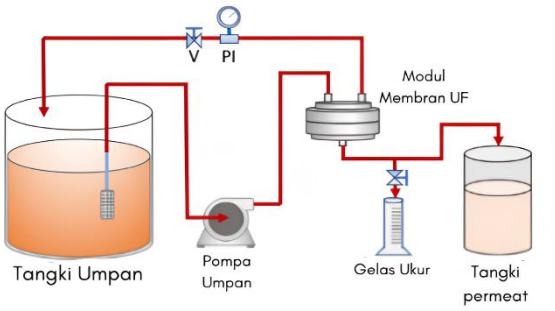

Figure 3. Schematic of Flux and Permeate Testing Equipment (Aryanti et al., 2022).

The selectivity of the membrane is expressed through a rejection value (R, in %), which is calculated using the following equation:

$$R\ (\%) = 1 - \frac{Cp}{Cf} x100\% \quad (4)$$

The variable C_p is the solute concentration in the permeate (pure water), while C_f is the concentration in the feed solution (raw water polluted with textile industry waste). To evaluate the tight-UF membrane resulted, testing was carried out using organic compound rejection. The concentration of organic compounds was measured using a UV-vis spectrophotometer at a wavelength of 254 nm *(Shi et al.*, 2022).

Morphological Analysis and Chemical Properties of Membranes

Membrane morphology was analyzed using a Scanning Electron Microscope (SEM, JSM-6510LV, low vacuum) at 500 – 1000× magnification. The dried UF membranes were immersed in liquid nitrogen, then broken to obtain a transverse view. The broken side of the membrane was coated with gold using a spray precipitator before being observed under the SEM unit.

Meanwhile, the observation of membrane chemical properties was conducted using Fourier Transform Infra-Red (FTIR). Before analysis, the Tight-UF membrane samples were dried for 3 days in a desiccator to remove water in the membrane structure.

Porosity Testing of Tight-UF Membrane

Membrane porosity (ε, %) was calculated using equation (5).

$$\varepsilon_0(\%) = \frac{\frac{W_w - W_d}{\rho_i}}{\left(\frac{W_w - W_d}{\rho_i}\right) + \left(\frac{W_d}{\rho_p}\right)} \times 100 \qquad (5)$$

where W_w is wet mass of the tight-UF membrane and W_d is the dry mass (in grams, g). Whereas ρ_i is the density of water (0.998 g·cm^{-3}) and ρ_p is the density of PSf (1.23 g·cm^{-3}). Before weighing, the tight-UF flat-sheet membrane was soaked in distilled water to ensure that all the pores of the tight-UF membrane were filled with water. The water on the membrane surface was gently dried using a tissue, then weighed. Next, the membrane was dried for 3 days in a desiccator to evaporate all the water from the membrane structure and then weighed.

Contact Angle Testing

The water contact angle at the membrane surface was measured using the sessile drop method. Distilled water was dripped over the ultrafiltration membrane surface using a microsyringe (syringe). The angle between the water drops and the membrane surface was analyzed using ImageJ software (version v1.53n). Measurements were taken 7× at various locations to minimize reading errors. The contact angle measurements are shown in Figure 4.

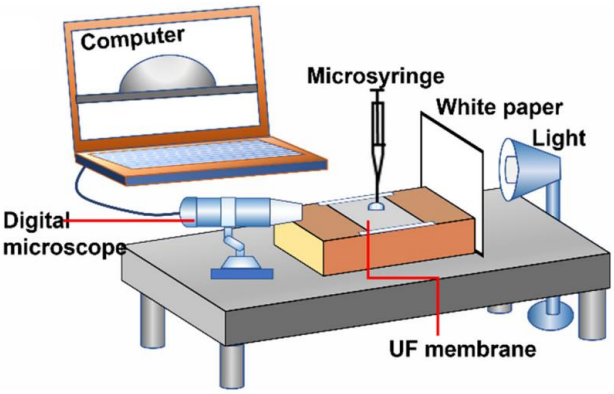

Figure 4. Contact angle measuring device *(Aryanti et al*., 2022)

RESULTS AND DISCUSSION

Morphology and Chemical Properties of SPSF/HNT/Acetone Ultrafiltration Membrane

Figure 5 presents cross-sectional SEM images of the tight-UF membranes fabricated with different casting solution compositions. Figure 5a shows the membrane prepared from sulfonated PSf using 70 wt.% sulfuric acid, with the addition of 20 wt.% PEG400 and 1 wt.% HNT in the absence of acetone (SPSf-70/PEG400/HNT/AC 20/20/1/0). The micrograph revealed the formation of relatively large pores extending throughout the membrane cross-section. This morphology can be ascribed to the combined effects of sulfonation and PEG400 addition. Sulfonation introduces hydrophilic –SO_3H groups into the polymer backbone, which increase affinity toward water and promote pore formation during phase inversion, while PEG400 acts as an effective pore-forming agent by generating interconnected voids.

Figures 5b and 5c show the influence of acetone addition on the membrane structure. Due to its high volatility, acetone enhanced the local polymer concentration at the membrane surface during casting, leading to the development of a denser and mechanically reinforced skin layer. At higher acetone loading (6 wt.%), the resulting structure appeared tighter, with reduced pore size and increased rigidity. This behavior suggests that rapid solvent evaporation accelerated the solvent–nonsolvent exchange and induced faster polymer precipitation. Such accelerated demixing constrained pore growth, yielding a more compact morphology, a phenomenon frequently reported for membranes prepared with volatile co-solvents.

Figure 5d shows the effect of increasing the sulfonation degree to 98 wt.% sulfuric acid (SPSf-98). The incorporation of sulfonate groups (-SO_3H) significantly enhanced the polarity and hydrophilicity of the polymer matrix, thereby facilitating water transport into the membrane structure. This increased hydrophilicity lowers the interfacial free energy between the polymer phase and water, enabling greater water uptake. Furthermore, the inclusion of PEG400 contributed to the formation of larger pores by producing microvoids during the phase inversion process. This phenomenon can be explained by the enhanced thermodynamic instability of the casting solution, where strong water–polymer interactions accelerate solvent–nonsolvent exchange and promote pore nucleation and growth.

Figure 5e shows that membranes prepared with higher HNT concentrations in the absence of acetone exhibited a looser polymer network and more accelerated phase separation, ultimately yielding larger pore sizes. This morphological evolution can be attributed to the synergistic effects of extensive sulfonation and HNT incorporation. The high concentration of HNT increased hydrophilicity and destabilized the polymer solution thermodynamically, facilitating rapid demixing and phase separation. The combined effect promoted the development of a more open porous structure and higher overall pore connectivity.

The chemical structure of the SPSf/PEG400/HNT membranes was analyzed using Fourier Transform Infrared (FTIR) spectroscopy, as shown in Figure 6. The broad absorption bands observed in the range of 3160 – 3600 cm^{-1} in both membrane types are attributed to O-H stretching vibrations, confirming the incorporation of PEG400 in the membrane matrix. The distinct absorption band at 1160 cm^{-1} corresponds to the symmetric stretching of sulfonate groups (-SO_3H), which verifies the successful sulfonation of PSf.

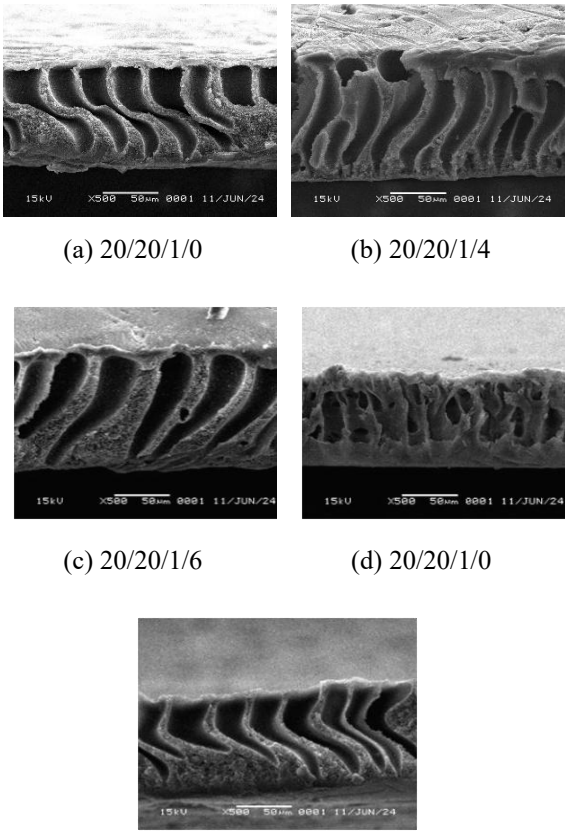

(a) 20/20/1/0 (b) 20/20/1/4

(c) 20/20/1/6 (d) 20/20/1/0

(e) 20/20/4/0

Figure 5. Scanning Electron Microscope (SEM) Cross-section of UF membrane at various concentrations of SPSf/PEG400/HNT/Ac.

In addition, the peak at 1725 cm^{-1}, detected in both membranes, is assigned to C=O stretching vibrations, indicating the presence of residual acetone and DMAc in the membrane structure (Smith, 2017). The absorption peaks detected at approximately 950 – 1255 cm^{-1} are typical features of HNT, corresponding to the Si-O-Si and Si-O-Al stretching vibrations (Can *et al*., 2021; Sedira and Castro-Gomes, 2020). The bands appearing between 674 and 412 cm^{-1} correspond to characteristic Al-OH and Si-O stretching vibrations, confirming the structural framework of the halloysite within the membrane matrix (Golubeva *et al*., 2020).

Table 1 presents the effect of membrane formulation on porosity for SPSf-70 and SPSf-98. The results indicate that the porosity of SPSf-98 is consistently higher than that of SPSf-70. This can be attributed to the stronger hydrophilic character imparted by the sulfonate ($–SO_3H$) groups, which enhances water affinity and facilitates pore formation during phase inversion. The presence of these functional groups lowers the interfacial free energy between the polymer matrix and nonsolvent, thereby promoting greater water penetration and generating a more open pore structure.

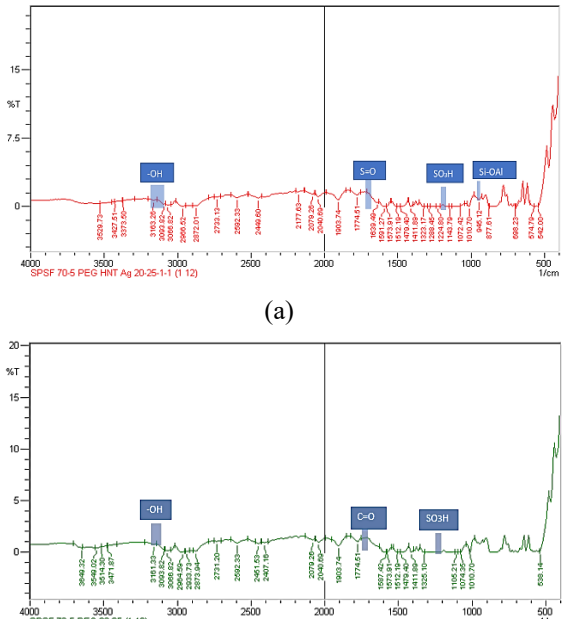

(a)

(b)

Figure 6. FTIR analysis results on membranes with composition: (a) SPSf-70/PEG400/HNT (b) SPSf-70/PEG400 Effect of Polymer Solution Formulation on Membrane Porosity

In contrast, increasing the concentration of acetone exhibits the opposite effect by reducing membrane porosity. For instance, in SPSf-70 with 1 wt.% HNT loading, raising the acetone concentration to 6 wt.% reduced porosity from 75.92% to 70.02% (a decrease of 7.77%). This reduction is explained by the rapid volatilization of acetone during membrane casting, which drives polymer aggregation toward the top layer and results in a denser surface. The accelerated solidification induced by solvent evaporation interrupts pore growth and suppressed phase separation, ultimately yielding smaller pore sizes and lower overall porosity.

Table 1. Porosity in Membranes

SPSf/PEG 400/HNT/AC (wt.%)	Membrane Porosity (%)	SPSf/PEG400/HNT/AC (wt.%)	Membrane Porosity (%)
70 20/20/1/0	75.92	70 20/20/2/0	71.16
70 20/20/1/4	73.63	70 20/20/2/4	68.18
70 20/20/1/6	70.02	70 20/20/2/6	65.45
98 20/20/1/0	78.40	98 20/20/2/0	74.55
98 20/20/1/4	76.31	98 20/20/2/4	71.75
98 20/20/1/6	74.01	98 20/20/2/6	69.42

Meanwhile, at SPSf-98 and the same HNT concentration (1 wt.%), the porosity decrease was 5.60%, from 78.40% to 74.01%. The lower porosity decreases in SPSf-98 compared to SPSf-70 is due to the hydrophilic nature of the membrane that allows water to enter the membrane pores, so that the membrane can still maintain the pore size along with the evaporation of the solvent (acetone). Increasing the HNT concentration to 2 wt.% resulted in a decrease in

membrane porosity. At higher concentrations, HNT tends to agglomerate or clump due to stronger inter-particle interactions. This agglomeration can disrupt the uniform distribution of HNT in the polymer matrix and fill more pore space, resulting in a smaller effective pore size of the membrane.

The Effect of Membrane Solution Formulation on Membrane Hydrophilicity

Membrane hydrophilicity was evaluated through water contact angle measurements using the sessile drop method. A membrane is generally classified as hydrophilic when the water contact angle is below 90° (Kronberg *et al*., 2014). Figure 7 shows the contact angle values of the tight-UF membranes with various compositions. All membranes exhibited contact angles below 90°, confirming their hydrophilic character. The highest contact angle, 73°, was observed for the SPSf-70 %/PEG400/HNT/Ac 20/20/2/0 membrane. This relatively higher value can be attributed to the dense polymer concentration near the membrane surface, further enhanced by acetone-induced surface compaction. Such densification reduces the exposure of hydrophilic functional groups (–SO_3H and –OH), thereby decreasing water affinity and increasing the contact angle.

In contrast, the lowest contact angles (63.8°–68.4°) were recorded for SPSf/PEG400/HNT/Ac 20/20/1/6 and 20/20/2/6 formulations, indicating superior hydrophilicity. This improvement arises from the synergistic contribution of sulfonated polysulfone (SPSf), which introduces –SO_3H groups capable of strong hydrogen bonding with water, and PEG400, which enhances pore formation and increases the exposure of hydrophilic domains. Additionally, higher acetone concentrations promote faster solvent–nonsolvent exchange, facilitating the migration of PEG and HNT toward the surface during phase inversion. Although this enhances surface hydrophilicity, it may simultaneously compact the sublayer, an effect later observed in the flux analysis.

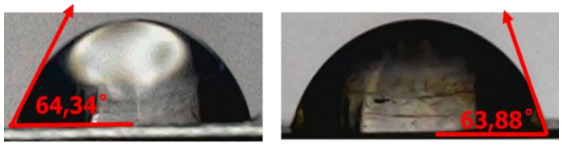

Figure 7. Contact angle measurement results (a) 70-SPSf 20 wt.%, HNT 1 wt.%, Acetone 6 wt.% (b) 98-SPSf 20 wt.%, HNT1 wt.%, Acetone 6 wt.%

Effect of Membrane Formulation on Sulfonation Degree and Permeate Flux

The degree of sulfonation (DS) of SPSf prepared with 70 w.t% and 98 wt.% H_2SO_4 is shown in Figure 8a, calculated using Equation (2) based on the ion exchange capacity (IEC) of the polymer. The DS value of SPSf-98 was found to be higher than that of SPSf-70. This difference is attributed to the higher concentration of H_2SO_4 in the 98 wt.% solution, which provides a greater availability of sulfonate ions (-SO_3H) to react with the PSf backbone. As a result, the sulfonation reaction proceeded more efficiently, yielding an increased number of -SO_3H groups covalently bound to the polymer structure. A higher DS enhances the polarity and hydrophilicity of the polymer matrix, which in turn facilitates water uptake and promotes more effective water transport through the membrane pores.

Figure 8b shows the permeate flux of SPSf-70/HNT/AC and SPSf-98/HNT/AC membranes during 60 minutes of filtration. The SPSf-98 membrane displayed a higher initial flux (73 $L \cdot m^{-2} \cdot h^{-1}$) than SPSf-70 (71 $L \cdot m^{-2} \cdot h^{-1}$), confirming that higher sulfonation improves hydrophilicity and water transport. However, both membranes experienced flux decline with time due to fouling. After 60 minutes, SPSf-98 and SPSf-70 retained 27 % and 24 % of their initial flux, corresponding to flux declines of 73 % and 76 %, respectively. Although SPSf-98 exhibited slightly higher flux loss numerically, its greater residual flux indicates improved fouling resistance, likely due to the formation of a negatively charged hydrated surface that repels organic foulants. Thus, controlling sulfonation level is essential to balance water affinity and morphological stability.

Figure 8c illustrates the influence of HNT loading (1 wt.% and 2wt %) on membrane flux performance. Increasing HNT concentration from 1 wt.% to 2 wt.% reduced initial flux and slightly accelerated flux decline. After 60 minutes, SPSf-70 membranes exhibited flux losses of 72–75 %, and SPSf-98 membranes exhibited 70–74 %. This reduction is attributed to nanoparticle agglomeration at higher loading, which blocks the pore and decreases effective porosity. Conversely, at moderate loading (1 wt.%), uniformly dispersed HNTs enhance hydrophilicity and create water channels through hydrogen bonding, improving both permeability and fouling resistance. Therefore, 1 wt.% HNT is considered optimal for achieving stable flux and structural uniformity.

The results in Figure 8d demonstrate the effect of acetone fraction (0, 4, and 6 wt.%) on membrane permeability. The membrane prepared without acetone exhibited the highest flux (75 $L \cdot m^{-2} \cdot h^{-1}$), while those with 4 wt.% and 6 wt.% acetone showed reduced fluxes of 65 and 63 $L \cdot m^{-2} \cdot h^{-1}$, respectively. After 60 minutes of operation, all membranes experienced 70 – 77 % flux decline. The decrease in flux with higher acetone content is attributed to its high volatility, which accelerates solvent evaporation and induces rapid polymer precipitation during casting. This creates a denser, less porous substructure that increases hydraulic resistance. While a higher acetone ratio improves surface hydrophilicity by promoting additive migration (as observed in contact-angle results), it simultaneously densifies the bulk structure, reducing pore interconnectivity and overall permeability.

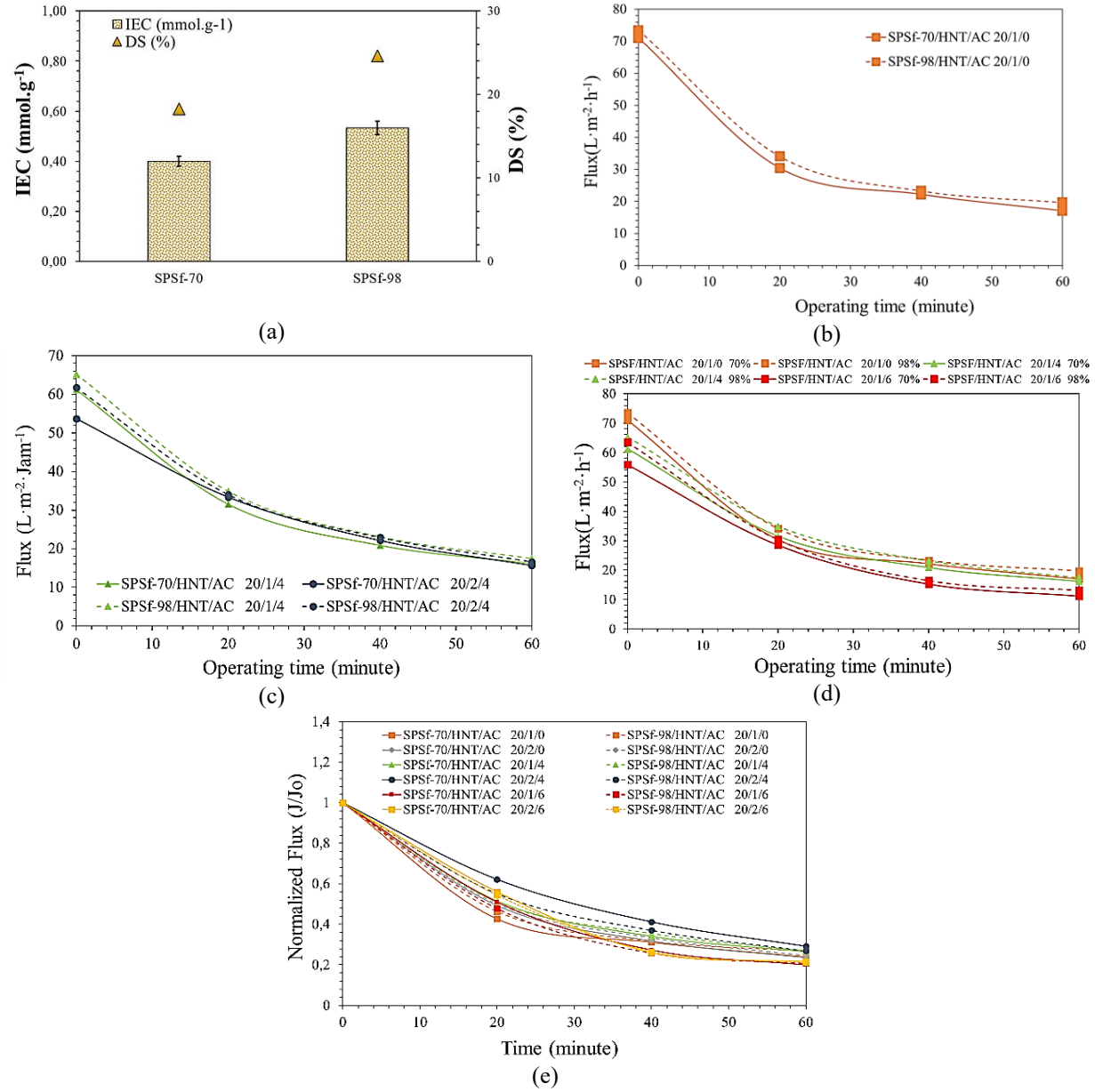

Figure 8. Research results on (a) sulfonation degree (DS) and the profile of permeate flux at: (b) various variations of SPSf, (c) various variations of HNT (d) various variations of acetone, and (e) flux decrease for 1 hour filtration time.

Hence, a moderate acetone ratio (≈ 4–6 wt.%) is optimal for balancing surface wettability and internal mass-transfer resistance.

Figure 8e displays normalized flux (J/J_0) versus filtration time. A rapid initial decline (40 – 50% within 20 minutes) reflects pore blocking by colloids and organic matter, followed by a slower decline due to cake-layer buildup. After 60 minutes, SPSf-70 membranes retained only 24 – 28% of their initial flux, whereas SPSf-98 membranes retained 30 – 35%, confirming superior antifouling properties. This improvement is attributed to abundant $–SO_3H$ groups on SPSf-98, which promote electrostatic repulsion and hydration-layer formation that hinder foulant attachment. The synergistic effect of PEG400 and HNT further enhances surface smoothness and hydrophilicity, reducing irreversible fouling. In overall, the optimized composition (SPSf-98/PEG400/HNT/Ac 20/20/1/6 wt.%) maintained the best balance between high initial flux (~63 $L \cdot m^{-2} \cdot h^{-1}$) and moderate flux decline (65 – 70%), representing a stable and energy-efficient tight-UF configuration suitable for sustainable water treatment applications.

The Effect of Membrane Formulation on Contaminant Rejection

Figure 9 illustrates rejection performance of organic compounds in river water. The membranes exhibited rejection efficiencies ranging from 86% to 98 %. The lowest rejection occurred for SPSf-

98/PEG400/HNT/Ac 20/20/2/0, while the highest (98 %) was achieved for SPSf-98/PEG400/HNT/Ac 20/20/2/6. The absence of acetone resulted in thinner skin layers and larger pores, decreasing the retention of small organics (~400 Da). Conversely, increasing the acetone concentration yielded thicker, denser selective layers, which enhanced size-exclusion and charge-repulsion effects, albeit at the expense of lower flux.

This trend complements the flux results (Figure 8d), confirming that acetone-induced densification enhances selectivity while reducing permeability. The SPSf-98/PEG400/HNT/Ac 20/20/1/6 wt.% membrane achieved the most balanced performance, namely high rejection (close to 98 %) with adequate flux (63.45 $L \cdot m^{-2} \cdot h^{-1}$), making it a promising candidate for advanced water purification and decentralized treatment systems.

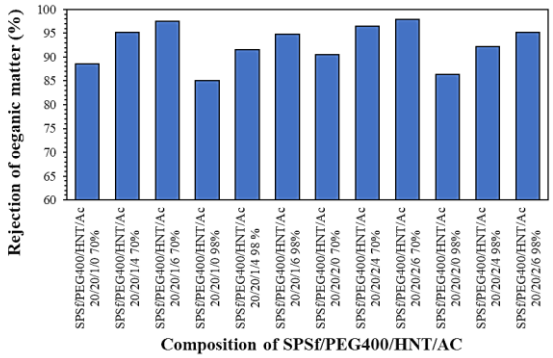

Figure 9. Rejection Parameters for Organic Compounds

CONCLUSION

Sulfonated polysulfone (SPSf)–based tight ultrafiltration membranes were successfully developed for treating raw water contaminated by industrial effluents. The effects of sulfonation degree, HNT loading, and acetone concentration on membrane structure and performance were comprehensively evaluated by characteristics and filtration analyses.

Increasing the sulfonation degree (from 70 to 98 wt.% H_2SO_4) improved the membrane's hydrophilicity and charge density, thereby enhancing the initial flux and fouling resistance. Moderate HNT incorporation (1 wt.%) further increased water permeability and surface stability by introducing hydrophilic nanochannels, whereas excessive loading (2 wt.%) led to agglomeration and partial pore blockage. Acetone has a dual effect: promoting additive migration that enhances surface wettability, but causing bulk densification and reduced porosity when used excessively.

Among all tested compositions, the SPSf/PEG400/HNT/Ac 20/20/1/6 wt.% membrane at 98 wt.% sulfonation achieved the most balanced performance, combining high organic rejection (98.5%) with sustainable flux (63.45 $L \cdot m^{-2} \cdot h^{-1}$) and moderate flux decline (between 65 to 70%). These results demonstrate that precise tuning of the sulfonation degree, additive ratio, and solvent composition enables the production of tight-UF membranes with optimal selectivity, stability, and energy efficiency for sustainable water purification applications.

ACKNOWLEDGEMENTS

The authors gratefully acknowledge the Directorate of Learning and Student Affairs, Ministry of Education, Culture, Research, and Technology of the Republic of Indonesia, for financial support provided through the Student Creativity Program–Research (PKM-RE), under Letter No. 2546/E2/DT.01.00/2024 dated 19 April 2024. The authors also extend their appreciation to the Student Affairs Division of Jenderal Achmad Yani University for institutional support.

REFERENCES

Akli, K., Khoiruddin, K. and Wenten, I., 2016. Preparation and characterization of heterogeneous PVC-silica proton exchange membrane. *Journal of Membrane Science and Research 2(3)*, 141-146. https://doi.org/10.22079/jmsr.2016.20312

Aryanti, P.T.P., Noviyani, A.M., Kurnia, M.F., Rahayu, D.A. and Nisa, A.Z., 2018. Modified Polysulfone Ultrafiltration Membrane for Humic Acid Removal During Peat Water Treatment. *IOP Conference Series: Materials Science and Engineering 288*, 012118. https://10.1088/1757-899x/288/1/012118

Aryanti, P.T.P., Nugroho, F.A., Widiasa, I.N., Sutrisna, P.D. and Wenten, I.G., 2022. Preparation of highly selective PSf/ZnO/PEG400 tight ultrafiltration membrane for dyes removal. *Journal of Applied Polymer Science 139(33)*, e52779. https://doi.org/10.1002/app.52779

Basuki, T.M., Indrawati, D.R., Setio Hadi Nugroho, H.Y., Pramono, I.B., Setiawan, O., Nugroho, N.P., Hilmya Nada, F.M., Nandini, R., Savitri, E. and Adi, R.N., 2024. Water Pollution of Some Major Rivers in Indonesia: The Status, Institution, Regulation, and Recommendation for Its Mitigation. *Polish Journal of Environmental Studies 33(4)*, 3515-3530. https://doi.org/10.15244/pjoes/178532

Can, M., Demirci, S., Yildrim, Y., Çoban, C.Ç., Turk, M. and Sahiner, N., 2021. Modification of halloysite clay nanotubes with various alkyl halides, and their characterization, blood compatibility, biocompatibility, and genotoxicity. *Materials Chemistry and Physics 259*, 124013. https://doi.org/10.1016/j.matchemphys.2020.124013

Chakraborty, S.K., 2021. Riverine Ecology Volume 2: Biodiversity Conservation, Conflicts and Resolution. Chakraborty, S.K. (ed), pp. 443-530, *Springer International Publishing*, Cham. https://doi.org/10.1007/978-3-030-53941-2_5

Choi, S., Chaudhari, S., Shin, H., Cho, K., Lee, D., Shon, M., Nam, S. and Park, Y., 2022. Polydopamine-modified halloysite nanotube-incorporated polyvinyl alcohol membrane for pervaporation of water-isopropanol mixture. *Journal of Industrial and Engineering Chemistry 105*, 158-170. https://doi.org/10.1016/j.jiec.2021.09.016

de Oliveira, A.D. and Beatrice, C.A.G., 2018. Nanocomposites-recent evolutions. Sivasankaran, S. (ed), *IntechOpen*, London, United Kingdom. https://doi.org/10.5772/intechopen.81329

Golubeva, O.Y., Alikina, Y.A. and Kalashnikova, T.A., 2020. Influence of hydrothermal synthesis conditions on the morphology and sorption properties of porous aluminosilicates with kaolinite and halloysite structures. *Applied Clay Science 199*, 105879. https://doi.org/10.1016/j.clay.2020.105879

Kalkhoran, H.M., 2015. Development of Blend Ionic Liquid Glassy Membrane for CO2/CH4 Gas Separation. *Dissertation, Universiti Teknologi Petronas, Malaysia*.

Katana, B., Takács, D., Csapó, E., Szabó, T., Jamnik, A. and Szilagyi, I., 2020. Ion Specific Effects on the Stability of Halloysite Nanotube Colloids—Inorganic Salts versus Ionic Liquids. *The Journal of Physical Chemistry B 124(43)*, 9757-9765. https://doi.org/10.1021/acs.jpcb.0c07885

Kronberg, B., Holmberg, K. and Lindman, B., 2014. Surface chemistry of surfactants and polymers, *John Wiley & Sons*.

Sedira, N. and Castro-Gomes, J., 2020. Low liquid-to-solid ratio of mining waste and slag binary alkali-activated material. *KnE Engineering*, 202–213-202–213. https://knepublishing.com/index.php/KnE-Engineering/article/download/6941/12615

Shi, Z., Chow, C.W.K., Fabris, R., Liu, J. and Jin, B., 2022. Applications of Online UV-Vis Spectrophotometer for Drinking Water Quality Monitoring and Process Control: A Review. *Sensors 22(8)*, 2987. https://doi.org/10.3390/s22082987

Siagian, U.W., Khoiruddin, K., Wardani, A.K., Aryanti, P.T., Widiasa, I.N., Qiu, G., Ting, Y.P. and Wenten, I.G., 2021. High-performance ultrafiltration membrane: Recent progress and its application for wastewater treatment. *Current Pollution Reports 7*, 448–462. https://doi.org/10.1007/s40726-021-00204-5

Smith, B.C., 2017. The carbonyl group, part I: introduction. *Spectroscopy 32(9)*. https://www.spectroscopyonline.com/view/carbonyl-group-part-i-introduction

Tang, Y.-h., Ledieu, E., Cervellere, M.R., Millett, P.C., Ford, D.M. and Qian, X., 2020. Formation of polyethersulfone membranes via nonsolvent induced phase separation process from dissipative particle dynamics simulations. *Journal of Membrane Science 599*, 117826. https://doi.org/10.1016/j.memsci.2020.117826

Wang, T., Wu, H., Zhao, S., Zhang, W., Tahir, M., Wang, Z. and Wang, J., 2020. Interfacial polymerized and pore-variable covalent organic framework composite membrane for dye separation. *Chemical Engineering Journal 384*, 123347.

Xiang, H., Min, X., Tang, C.-J., Sillanpää, M. and Zhao, F., 2022. Recent advances in membrane filtration for heavy metal removal from wastewater: A mini review. *Journal of Water Process Engineering 49*, 103023. https://doi.org/10.1016/j.jwpe.2022.103023

Xie, T., Li, F., Chen, K., Zhao, S., Chen, Y., Sun, H., Li, P. and Niu, Q.J., 2023. Fabrication of novel thin-film nanocomposite polyamide membrane by the interlayer approach: A review. *Desalination 554*, 116509. https://doi.org/10.1016/j.desal.2023.116509